IRIS AperTO

UNIVERSITÀ DEGLI STUDI DI TORINO

AperTO - Archivio Istituzionale Open Access dell'Università di Torino

Blocking layer optimisation of poly(3-hexylthiopene) based Solid State Dye Sensitized Solar Cells

This is the author's manuscript

Original Citation:

Availability:

This version is available http://hdl.handle.net/2318/139694 since 2016-10-10T10:22:02Z

Published version:

DOI:10.1016/j.orgel.2013.03.037

Terms of use:

Open Access

Anyone can freely access the full text of works made available as "Open Access". Works made available under a Creative Commons license can be used according to the terms and conditions of said license. Use of all other works requires consent of the right holder (author or publisher) if not exempted from copyright protection by the applicable law.

(Article begins on next page)

13 May 2024

IRIS AperTO

UNIVERSITÀ DEGLI STUDI DI TORINO

This Accepted Author Manuscript (AAM) is copyrighted and published by Elsevier. It is posted here by agreement between Elsevier and the University of Turin. Changes resulting from the publishing process - such as editing, corrections, structural formatting, and other quality control mechanisms - may not be reflected in this version of the text. The definitive version of the text was subsequently published in ORGANIC ELECTRONICS, 14 (7), 2013, 10.1016/j.orgel.2013.03.037.

You may download, copy and otherwise use the AAM for non-commercial purposes provided that your license is limited by the following restrictions:

(1) You may use this AAM for non-commercial purposes only under the terms of the CC-BY-NC-ND license.

(2) The integrity of the work and identification of the author, copyright owner, and publisher must be preserved in any copy.

(3) You must attribute this AAM in the following format: Creative Commons BY-NC-ND license (http://creativecommons.org/licenses/by-nc-nd/4.0/deed.en), 10.1016/j.orgel.2013.03.037

The publisher's version is available at:
http://linkinghub.elsevier.com/retrieve/pii/S1566119913001511

When citing, please refer to the published version.

Link to this full text:
http://hdl.handle.net/2318/139694

This full text was downloaded from iris - AperTO: https://iris.unito.it/

iris - AperTO

University of Turin's Institutional Research Information System and Open Access Institutional Repository

Blocking Layer Optimization of poly(3-hexylthiopene) based Solid State Dye Sensitized Solar Cells

F.Matteocci[1], G. Mincuzzi[1], F. Giordano[1], Emma Artuso[2], C. Barolo[2], G. Viscardi[2], T.M. Brown[1], A. Reale[1], A. Di Carlo[1,(*)]

1. *C.H.O.S.E. (Centre for Hybrid and Organic Solar Energy), Department of Electronic Engineering,, University of Rome "Tor Vergata",via del Politecnico 1, Rome, 00133 Italy*
2. *Department of General and Organic Chemistry, University of Torino, via P. Giuria 7, Torino, 10125 Italy*

[(*)]E-mail: aldo.dicarlo@uniroma2.it

Abstract

The optimisation study of a compact TiO_2 blocking layer fabrication (via Spray Pyrolysis Deposition) for poly(3-hexylthiopene) (P3HT) based Solid State Dye Sensitized Solar Cells (SDSC) is reported. We used a novel spray TiO_2 precursor solution composition obtained by adding acetylacetone to a conventional formulation (Diisopropoxytitanium bis(acetylacetonate) in ethanol). By Scanning Electron Microscopy a TiO_2 layer with compact morphology and thickness of around 100 nm is shown. Through a Tafel plots analysis an enhancement is observed of device diode-like behaviour induced by the acetylacetone blocking layer respect to the conventional one. Significantly, device fabricated with acetylacetone blocking layer shows an overall increment of the cell performances respect to cell with conventional one ($\Delta J_{sc}/J_{sc}$= +13.8%, ΔFF/FF= +39.7%, ΔPCE/PCE= +55.6%). A conversion efficiency optimum is found for successive spray cycles n = 15 where more effective is the acetylacetone blocking layer diode-like behaviour. Over three batches of cells (fabricated with P3HT and dye D35) an average conversion efficiency value of 3.9% (under a class A sun simulator with 1 sun A.M. 1.5 illumination condition) was measured. From the best cell we fabricated a conversion efficiency value of 4.5% was extracted. This represent a significant increment respect to previously reported values for P3HT/ dye D35 based SDSC.

Keywords: solid state dye sensitized solar cell; compact layer TiO_2; poly(3-hexylthiopene); organic dye; spray pyrolysis deposition.

1. Introduction

Owing to the use of potentially low cost materials and relatively easy fabrication processes, Dye-Sensitized Solar Cells (DSCs) are an attractive photovoltaic technology candidate for large scale production [1,2]. A basic DSC configuration is obtained juxtaposing between two conductive and transparent substrates (generally FTO/glass) a nanocrystalline TiO_2 film (n-TiO_2) sensitized to the visible light by means of an absorbing dye (attached on the nanocrystals surface) a liquid electrolyte (a redox couple in a liquid solvent) and a catalytic layer (conventionally made of Pt). Large area devices are obtained interconnecting single cells. An electron injected from the dye into the n-TiO_2 film after dye photoexcitation diffuses through the substrate and an external load, generating electrical power. Finally the electron is again available for the dye regeneration through a redox reaction (catalysed by the Pt).

Although a conversion efficiency (PCE) value higher than 12.3% has been reached over small area [3] several demanding issues should be addressed before the commercial exploitation of DSC technology [4-7].

Here we mention in particular the increase of device life time and long term stability which is, amongst the other, connected to the mechanical, and electrochemical stability of the liquid electrolyte. In fact, being the latter extremely volatile (is conventionally composed by the redox couple I_3^-/I^- and a solvent such as MPN, ACN or VN) DSC devices suffer from leakage induced problems like insufficient ionic diffusion current and corrosion of metallic contacts [8-9]. Furthermore it has been shown that in reverse bias conditions liquid electrolyte will deteriorate with consequent fatal effects on the cell performances [10]. Several alternative strategies have been proposed to tackle these issues including the use of less corrosive redox couple (such as C_O(II) C_O(III)), solvent free electrolyte and polymer gel electrolyte [3,11-14]. Highly promising are the so called Solid State DSC (SDSC) where the electrolyte is replaced by an hole transporter material (HTM) with the straightforward advantage of overtake all the here mentioned problems [15-18]. Being in SDSC the electron recombination rate at the interface n-TiO_2/HTM higher than n-TiO_2/electrolyte, dye regeneration is optimized reducing the n-TiO_2 thickness (down to few μm) which the drawback to reduce the device light harvesting [19-20]. In this case, dyes with an high extinction molar coefficient ε (such as the tri-arylamine-based D35 Dye with ε = 30000 mol^{-1}) have been shown to have a positive impact on the device performances [21-23].

High performances have been obtained using an organic, transparent, p-type doped, small molecule compound called Spiro-OMETAD, although the high production cost makes its employment prohibitive for large area devices [19-23]. Very recently a PCE = 10.2% has been measured from a SDSC (in which photonic crystals were embedded) using a p-type inorganic semiconductor $CsSnI_3$ (HTM) and Ru-based dye (N719) [24]. Amongst organic HTM compounds, P3HT is a promising

option in order to obtain high performing SDSC devices [25-29]. In fact, its hole conductivity may be higher respect to pristine Spiro-OMeTAD [28] making it a promising and cost effective alternative to Spiro-OMETAD. Snaith et al. have shown that by an accurate engineering of the interface TiO_2/P3HT promising performance can be obtained (PCE=2.81%) [27]. Hagfeldt and co-authors extracted from a cell using a P3HT/ dye D35 a PCE=3.2% [28]. It has been shown that for SDSC, holes (in the HTM) and FTO surface electrons recombination processes originates a remarkable current leakage path (back transfer) [30-32]. It becomes therefore crucial in SDSC device fabrication to engineer a compact (c) blocking layer (BL) between FTO/n-TiO_2 with the aim to induce a diode like behaviour (or current rectification) consisting in a drastic reduction of the back transfer recombination rate but letting the photo-extracted electrons to be efficiently collected. Several techniques have been utilized for the BL fabrication, including Magnetron Sputtering, Atomic Layer Deposition, Sol-Gel Process and Electrodeposition [26, 33-35], although, for a low cost processing, Spray Pyrolysis Deposition (SPD) of a precursor solution (conventionally consistent of Diisopropoxytitanium bis(acetylacetonate) dissolved in a solvent such as isopropyl alcohol or EtOH) is a prominent option and a nearly 100 nm thick c-TiO_2 layer is conventionally adopted as an optimum condition [29-31]. It has been shown that the thickness, morphology and electromechanical bonding with respect to the upper and lower interfaces are the key parameters to optimise, having a huge bearing on the BL electrical properties and therefore on the final device performance [36-37].

Here for the first time a c-TiO_2 BL was fabricated by SPD technique utilising a novel precursor composition obtained by adding acetylacetone (ACAC) to Diisopropoxytitanium bis(acetylacetonate) hereinafter referred as ACAC-BL. By Scanning Electron Microscopy (SEM) we show not only that a TiO_2 film with a compact morphology is obtained but also that P3HT is uniformly interpenetrated all along the n-TiO_2. Moreover, by Tafel plot analysis an enhancement is observed of the BL rectifying properties.

In fact, compared to conventional BL, both a lower value of the exchange current I_0 (indicative of the BL thickness, morphology and interface adhesion) and a lower anodic transfer coefficient β_a (proportional to the transfer resistance at the interface nc-TiO_2/HTM) were observed.

Furthermore average values of electrical parameters (J_{sc}, V_{oc}, PCE, FF) measured from a batch of cells fabricated with a ACAC-BL were compared with those extracted from a second batch of cells fabricated with a conventional BL. In spite of a negligible variation of V_{oc} ($\Delta V_{oc}/V_{oc}$= -1.8%) a remarkable enhancement is observed for the value of J_{sc} ($\Delta J_{sc}/J_{sc}$= +13.8%) and even more of FF ($\Delta FF/FF$= +39.7%) resulting in an overall increase of the PCE value ($\Delta PCE/PCE$= +55.6%).

The whole SPD process for ACAC-BL fabrication in SDSC was shown to observe an optimum in term of final device PCE when the number of successive SPD spray cycles n = 15.

Tafel plot analysis indicates that in correspondence of n = 15 not only the thickness of the BL reached an effective value but also shows optimal rectifying properties (high β_c and low β_a). By

Electro Impedance Spectroscopy (EIS) analysis the variation of the FTO surface left uncovered by BL obtained with various *n* and for both precursor composition has been analysed. Finally from three batches of cells fabricated with P3HT/D35, an ACAC-BL and *n* = 15 an average PCE value higher than 3.7% was extracted (for batch iv, v and vi) and IPCE measurements were carried out on a representative device showing a PCE=3.9%. The best cell we fabricated shows a PCE=4.5% which is a significant improvement respect to all previously reported values for SDSC utilising the same set of materials.

2. Experimental

FTO/glass substrates (Pilkington, 15 Ω/□, 25mm × 25mm) were etched via raster scanning laser ($Nd:YVO_4$ pulsed at 30 kHz average output power P=10 W) to form the desired electrodes pattern. 4 cells were formed on each substrate. Patterned substrates were cleaned with detergent, de-ionized water and ethanol, in an ultrasonic bath. By SPD technique a c-TiO_2 film was deposited onto FTO surface. During the deposition the substrate temperature was fixed at 450°C, the distance between the substrate positioned flat and the aerograph (tilted about 45° respect to the substrate) was fixed to 20 cm. To let an effective pyrolysis of TiO_2 precursor solution we waited 10 s before to carry out the successive spray cycle [30]. Number of successive spray cycles *n* was varied between 0 (i.e. no BL) and 50. Six batches of cells were fabricated with the same set of materials but with different BL. Batch (i) consisted of two set of 3 cells each. For the first set the composition of the precursor spray solution consisted of 0.16M Diisopropoxytitanium bis(acetylacetonate) (TAA) in 0.16M ethanol, whilst for the second set the composition consisted of 0.16 M TAA and 0.4 M ACAC in ethanol. In both cases was *n* = 15. Batch (ii) consisted of 4 sets of 3 cells. For all the sets the same precursor spray solution (0.16 M TAA and 0.4 M ACAC in ethanol) was utilised whilst for each set a different *n* value was utilised. In particular *n* was fixed to 0 (i.e no BL), 15, 30, 50. Batch (iii) was the same than batch (ii) except for the *n* values corresponding to each set. In this case was *n* = 5, 10, 15, 20. Finally, batches (iv), (v) and (vi) consisted of 3 cells each, with the same spray solution as for batch (ii) and *n* = 15.

Onto the substrates (with or without BL) was screen-printed a layer of TiO_2 nanoparticles based paste (18NR-T paste, Dyesol) successively subjected to a sintering process with a final step at 480°C for 30 min. The final thickness of the n-TiO_2 film was measured via profilometer (Dektak Veeco 150) to be 1.8 µm. n-TiO_2 films were dipped in a 40mM $TiCl_4$ aqueous solution for 30 min at 70 °C. After dipping samples were rinsed with deionized water and ethanol and then sintered at 500 °C for 30 min. n-TiO_2 films were subsequently sensitized by impinging (for 2 hours) in an organic dye (D35) solution (0.2mM in ethanol). D35 organic dye was synthetized as reported in the literature [41].

After being rinsed in ethanol and dried with air flow, substrates were dipped for 5 min into a

$LiN(CF_3SO_2)_2N$ (6 mg/mL, Aldrich) and 4-tert-butylpyridine (TBP, 30 mg/mL, Aldrich) solution in acetonitrile successively dried in air flow. Dye-sensitized n-TiO_2 films were spin coated with P3HT solution in chlorobenzene (Rieke Met. Inc. 15mg/mL, MW 30000-60000) making use of the following parameters: 40 s waiting time prior the deposition, 600 rpm for 12 s and finally at 1000 rpm for 40 s. Samples were introduced into a high vacuum chamber (10^{-6} mbar) in order to evaporate Ag back contacts (thickness 100 nm) by thermal evaporation. A device area of 0.25 cm^2 was defined by an evaporation mask.

Masked devices were tested under a solar simulator (ABET Sun 2000, class A) at AM1.5 and 100 mW/cm^2 illumination conditions calibrated with a Skye SKS 1110 sensor [42]. Incident photon-to-current conversion efficiency (IPCE) was measured using an apparatus consistent of an amperometer (Keithley 2612) and a monochromator (Newport Mod. 74000). Finally, Tafel characterization was performed by a potentiostat (Autolab PGSTAT 302N) using a scan rate of 1mV/s. Tafel plot analysis was carried out on complete devices in dark with an overpotential value (ΔE) varying in a wide range ($-0.7\ V<\Delta E<+0.7V$). Tafel Plot linear fittings were carried out in the high overpotential region for anodic and cathodic reactions ($|\Delta E| > 0.3V$).

A batch of symmetric cells (vii) was also fabricated. In this case, cells were obtained sealing together (by means of a thermoplastic gasket Bynel 60 μm thick) two identical FTO/Glass substrates coated with a c-TiO_2 layer. The c-TiO_2 layer (0.7 cm × 0.7 cm) was obtained via spray pyrolysis according to the procedure described above. Two different sets of symmetric devices were manufactured: for the first a conventional TiO_2 precursor solution was utilised whilst for the second we used an ACAC-TiO_2 precursor solution. In both cases the number of spray cycles n was varied and fixed to n = 0, 5, 15, 25. The c-TiO_2 layer was in turn uniformly coated with a Pt layer. The last was obtained subjecting to a temperature ramp with a final step of 5 min at 400 °C a Pt precursor solution (Platisol Solaronix) deposited via brush over the c-TiO_2 layers. Finally cells were completed injecting an electrolyte (HSE Dyesol).

Electro Impedance Spectroscopy Measurements were carried out in dark on batch (vii) devices in the frequency range between 300 kHz and 100 mHz with a bias potential $V_b = 0$ V. Spectra were successively fitted with the equivalent circuit R_s (R_{ct} Q) where is R_s the electrodes series resistance, R_{ct} and Q respectively the charge transfer resistance and the pseudo-capacitance at the Pt/FTO interface. The thickness and morphology of c-TiO_2 were evaluated from field emission scanning electron microscopy micrograph (Jeol JSM-7100F FE-SEM).

Finally Raman Spectroscopy analysis was carried out (by means of a micro-Raman System LabRAM ARAMIS provided by Horiba) on both conventional and ACAC blocking layers in the range of Raman Shifts 0-1800 cm^{-1}.

3. Results and Discussion

3.1 Optimisation of the c-TiO2 blocking layer processing. Firstly it worth observing that results of Raman Analysis carried out on both a conventional bl and an ACAC-BL (not shown here) reveals the presence of characteristic anatase TiO_2 footprint with a three peaks feature nearly around the Raman Shifts at 144 cm^{-1}, 514 cm^{-1} and 638 cm^{-1} [43, 44]. On the contrary, no one of rutile-TiO_2 characteristic foot-print peaks (in correspondence of the Raman shifts at 240 cm^{-1}, 443 cm^{-1} and 610 cm^{-1}) has been observed.

Relative variation of average electrical characteristic parameters (J_{sc}, V_{oc}, FF and PCE) measured from batch (i) devices with an ACAC-BL with respect to those with a BL without ACAC (hereinafter referred as conventional) are reported in fig.1. Albeit no appreciable variation is measured for V_{oc} ($\Delta V_{oc}/V_{oc}$= -1.8%±5.8%) remarkable relative increments are observed for all the remaining parameters and in particular $\Delta J_{sc}/J_{sc}$= 13.9 %±9.1%, ΔFF/FF= 39.7%±5.8%, ΔPCE/PCE= 55.6%±14.5%).

The overall enhancement of device performance can be ascribed to a better electromechanical adhesion of the c-TiO_2 layer on the FTO coated substrate [37-39]. In fact, it has been reported that Acetylacetonate groups plays a key role by inducing a functionalization of the FTO surface, aiding in turn an efficient attaching of the c-TiO_2 [39].

In particular, addition of acetylacetone into a Ti-isopropoxide solution has been demonstrated to induce the replacement of isopropoxide groups by chelating ACAC groups. The ACAC group bonded to Ti reduce the hydrolysis reaction rate with effect on the condensation pathway [45,46]. Moreover, Boland et al. have also shown that the effect is optimized when the molar ratio ϱ between ACAC and TiO_2 precursor is fixed between 2 and 3. When i ϱ < 2, a rapid precipitation of TiO_2 has been observed indicating that the titanium precursor was not fully stabilized. Whereas, when ϱ > 3 an excess of acetylacetonate groups after chelation leads the formation of TiO_3. This effect has been proved by FTIR analysis [45]. In our work we considered a value of ϱ = 2.4 which is quite in the middle of the optimum range [2,3]. Therefore by adding ACAC in BL for SDSC manufacturing not only will reduce the series charge transfer resistance in correspondence of the FTO/c-TiO_2 interface (with a positive impact on the device FF) but will also inhibit the recombination pathways at FTO/c-TiO_2 interface with a consequent enhancement of the extracted current. This effect was confirmed by extracting both series and shunt resistance of representative devices of batch (v) (as the inverse of the slope of the cell JV curve linear fit in correspondence of respectively V_{oc} and J_{sc} and referred respectively as r_s and r_{sh}). It can be observed that although r_s is kept nearly unchanged (respectively 96Ω 99Ω for conventional and ACAC device) a remarkable increment (from 3.33 to 8.33 kΩ) is observed for r_{sh} when passing from a conventional BL to an ACAC-BL. A further step required for a complete optimization of the ACAC-BL fabrication process for SDSC is the optimization of the SPD process parameters. These very likely will change with the set of materials utilised and in particular with the composition of the sprayed precursor

solution. A crucial parameter to gauge is the number of successive spray cycles *n*. This in fact will determine the film thickness and morphology having in turn a huge bearing on the final device performance [31]. A systematic study was carried out of the final device performance, and in particular of the PCE, vs. *n* varied over a wide range from *n* = 0 (i.e. the reference case where no BL are utilised) to *n* = 50. Fig.2 shows the PCE values extracted from devices of batch (ii) vs. *n* and reported normalised to the PCE value relative to *n* = 15. Starting from *n* =0 the efficiency is low and increases rapidly reaching a maximum for n =15 which is ten time the value relative to n =0. Increasing further the number of spray cycles (n > 15) the PCE drops off reaching a value which is only 10% of the maximum. Also reported (in fig.2) the PCE values extracted from cells of batch (iii) fabricated with an n value varying in a restricted range around n = 15 ($5 \leq n \leq 20$). Again, an optimum condition is found in correspondence of n = 15. It is interesting to observe that around the peak a smooth PCE trend is observed ($\Delta PCE/PCE < 14\%$ when is $10 \leq n \leq 20$) which is a suitable feature for a fabrication process to be candidate in an industrial environment.

In fig.3 is reported a SEM micrograph of a representative c-TiO2 film obtained by SPD after 15 spray cycles of the precursor solution containing ACAC. It can be observed that the film has a very irregular shape which roughly follows the underlaying substrate morphology. Large and highly necked aggregates can be distinguished determining a very compact film morphology. A film thickness $\delta \approx 100$ nm can be evaluated. This turns out to be consistent with all the previously reported studies relative to the thickness optimization of c-TiO2 BL but without ACAC where an optimum of $\delta \approx 80$ - 120 nm was found [30].

SEM micrograph reported in fig.4 shows a cross-section of the nc-TiO_2 film after dyeing and P3HT filling. A quasi continuous network of large aggregates with size of some hundreds of nanometers is easily distinguishable (highlighted with black dashed circles). According to [28] and [47] such large aggregates can be identified with the infiltrated P3HT polymer interpenetrating the nc-TiO_2 film (which in turn is composed of distinguishable nanoparticles with a size of around 20 nm). The uniform distribution (bottom, middle, up) of the large aggregates all along the entire film thickness can be reasonably assumed as the evidence that an uniform pore filling occurred into our nc-TiO_2 film.

3.2 Tafel Plots and Electro Impedance Spectroscopy. In this section we will make use of Tafel plots to study the BL-role plays in modifying the charge transfer properties between P3HT and FTO surface and the relation with final SDSC device perfomances. This study will provide an evaluation of how effective is the diode-like behaviour induced by the BL and resulting in a rectification of the cell's I-V characteristic. In particular it will enable to retrieve the values of the exchange current density I_0 and the cathodic and anodic transfer coefficient β_A and β_C relative to the Butler-Volmer equation.

$$I = -I_0 \left[e^{\frac{\beta_C nF}{RT}(E-E_{eq})} - e^{\frac{-\beta_A nF}{RT}(E-E_{eq})} \right]$$

Here I is total current, E the applied voltage, E_{eq} the P3HT electrode potential at equilibrium, n the number of electrons transferred. From an ideal BL is expected an extremely low value for β_a which guarantees a low charge transfer resistance at the n-TiO_2/FTO interface for photo-extracted charges and an extremely high β_c to stop the back transfer reaction. Finally I_0 depends on the BL thickness and morphology as well as on BL electromechanical adhesion properties respect to interfacing layers.

In Tab.1. the values of I_0, β_a, and β_c extracted from two representative cells of batch (i) having a BL fabricated with and without ACAC, are reported and compared. It can be observed that the addition of ACAC induces an enhancement of the diode-like behavior of the cell since it determines a relative β_a decrement of nearly 15% (from 231 $mV \cdot dec^{-1}$ to 198 $mV \cdot dec^{-1}$) whilst β_c is kept unmodified. Furthermore, the use of ACAC determines a I_0 reduction of about three order of magnitude which accounts very likely for the above mentioned improvement of the c-TiO_2 adhesion over the FTO. In fact a stronger adhesion will reduce the back transfer reaction area which in turn determine a reduction of I_0 [26].

In fig. 5 are reported the I_0, β_a and β_c values relative to a representative set of batch (iii) devices vs.*n*. Varying *n* from *n* =0 to *n* =15, I_0 (red squares) drops off drastically passing from $5.4 \cdot 10^{-5}$ A to $8.2 \cdot 10^{-7}$ A whilst, increasing the number on spray cycles ($n \geq 15$) it does not change significantly (maximum variation less than one order of magnitude). An effective thickness δ is reached already for *n* =15 blocking the exchange current at the FTO/c-TiO_2/P3HT interfaces. By increasing *n*, although will supposedly increase the film thickness does not induce a significant further reduction of I_0.

In the same fig. 5 the diode-like behaviour of the same devices are evaluated by means of the parameters β_a (back triangles) and β_c (green circles). As well as I_0, not only β_c values observe a remarkable variation passing from *n* = 0 to *n* = 15 (meaning that a significant block of the cathodic current associated to the back transfer recombination processes has been induced) but, increasing further *n* will not sensibly impacts the β_c value.

Importantly, the β_a value observe a sensible variation with respect to the cell without BL only when is $n \geq 30$ whilst in correspondence of *n* =15 it is similar to the value relative to *n* = 0 meaning that the anodic current (associated to the photo-extracted electrons current) is not reduced by the BL. The conclusion is straightforward in the sense that the diode-like behaviour of a c-TiO_2 ACAC-BL is optimised in correspondence of *n* =15. This consistently impact on the final devices performance resulting in the above reported PCE maximum observed when is *n* =15.

Interestingly, by EIS measurements carried out on batch (vii) (see experimental section) we also

evaluate how the portion of FTO surface Σ left uncover by the c-TiO_2 varies when varying *n* and the precursor solution composition. In fact, it can be reasonably asserted that in correspondence of Σ the Pt will adhere directly over the FTO letting an exchange current to flow into the cell with a charge transfer resistance R_{ct}. The R_{ct} value can be extracted fitting EIS spectra with the equivalent circuit model of figure below where R_s is the electrodes series resistance, R_{ct} the charge transfer resistance and Q the pseudo-capacitance at the Pt/FTO interface. Moreover R_{ct} is proportional to Σ according to the following:

$$R_{ct}/2 = r_{ct}/\Sigma \quad (1)$$

where the factor 2 is introduced to account for the two symmetric electrodes and the charge transfer resistance per unit surface r_{ct} ($\Omega \cdot cm^2$) is a constant which depend mainly on the electrolyte and Pt deposition method. Here the contribution of the c-TiO2 related resistance has been neglected considering that EIS measurement are performed at zero bias potential [48].

For our experiment, in correspondence of $n = 0$ (no c-TiO_2 layer) Σ = 0.7 cm × 0.7 cm (see experimental part) and an $R_{ct} \approx 80\ \Omega$ has been extracted leading to a value of $r_{ct} \approx 20\ \Omega \cdot cm^2$.

In fig. 6 are reported the EIS spectra of the symmetric cells for different *n* values and for the two c-TiO_2 precursor composition considered, conventional (open squares) and ACAC (open triangles). Increasing *n*, R_{ct} increases for both formulations assuming values which are quite similar. This is confirmed in the inset of fig. 6 showing in particular the values of Σ calculated according to eq. (1) and reported as percentage of the whole electrode surface (0.7 cm × 0.7 cm). When $n = 5$ the uncovered percentage of the whole electrode surface is lower than 16% and is reduced to nearly 1% for $n = 25$. In correspondence of the optimum $n = 15$, Σ = 3.5%.

In conclusion, EIS analyses of symmetric cells with platinized C-TiO2, show that, although the *n* value affect Σ, no significant differences are observed in terms of surface coverage between the two precursor formulation considered.

3.3 IPCE measurements of highly efficient devices. In order to evaluate the repeatability of the BL fabrication process here reported, three batches of cells (iv), (v) and (vi) were fabricated in the same experimental conditions with the same set of materials and a ACAC c-TiO_2 BL obtained with the value of $n = 15$ correspondent to the PCE optimum.

In fig. 7 are reported the average PCE values extracted from the three batches (iv), (v) and (vi). which are respectively equal to PCE= 3.8 % ± 0.7 % , PCE= 4.2 % ± 0.4 %, PCE= 3.7 % ± 0.2%. Interestingly all the average values calculated from the three batches of cells are higher than 3.2%

which is the highest reported for SDSC utilising the same set of active materials we used [28]. In fig. 8 is reported the IPCE spectrum extracted from a 3.94% efficient, representative cell (V_{oc}=847mV, J_{sc}= 7.18mA·cm^{-2} FF=64.77%). Importantly a maximum value approaching 70% is observed in correspondence of the dye absorption peak and, by integrating the IPCE curve from λ_1=300nm nm to λ_2=800nm we calculated a value of J_{sc}= 6.7 mA·cm^{-2}. The discrepancy respect to the value of J_{sc} measured under the sun simulator (< 8%) is very likely caused by the different intensity and spectral illumination conditions utilised during the IPCE measurements.

These results, confirmed over three batches of cells, demonstrate the reliability of the fabrication processes here reported for the SDSC BL. Finally from the best SDSC a PCE= 4.5% was extracted (see Fig.9) which is a further significant enhancement respect to the previously reported values for SDSC fabricated with the same set of materials.

4. Conclusion

Adding ACAC into a conventional precursor solution for c-TiO_2 layers fabrication (via SPD) utilised as BL in SDSC has been shown to determine an enhancement of the BL induced diode-like behaviour of the cell. In fact, ACAC enhances the c-TiO_2 adhesion over the FTO reducing the charge transfer resistance at the interface FTO/c-TiO_2. This in turn has a remarkable, positive impact on the final device performance. Under 1 sun, A.M. 1.5 illumination condition, relative increments (with respect to device with a conventional BL) were observed for J_{sc}, FF and PCE ($\Delta J_{sc}/J_{sc}$= +13.8%, ΔFF/FF= +39.7%, ΔPCE/PCE= +55.6%).

For this new precursor formulation a SPD process optimisation study was carried out by varying the number of successive spray cycles *n* over a wide range of values ($0 \leq n \leq 50$). An optimum, in term of final device PCE, has been found in correspondence of n = 15. Tafel parameters (I_0, β_a and β_c) show, in correspondence of the optimum, an enhancement of the SDSC diode-like behaviour (relatively low value of both I_0 and β_a and high β_c). Finally from three batches of cells fabricated with P3HT, dye D35 and an ACAC-BL with n = 15, an average PCE value higher than 3.7% was extracted (PCE= 3.8 % ± 0.7 %, PCE= 4.2 % ± 0.4 %, PCE= 3.7 % ± 0.2% respectively for batches (iv), (v) and (vi)). From IPCE measurements carried out on a representative device showing a PCE= 3.9 % a J_{sc}= 6.7 mA·cm^{-2} was extracted (after IPCE spectrum integration from λ_1 = 300 nm to λ_2 = 800 nm) which is compatible with the value extracted from the same cell under the sun simulator J_{sc}= 7.2 mA·cm^{-2}. Finally, from the best cell we fabricated a PCE=4.5% was extracted. This represent a significant improvement respect to previously reported value for SDSC using the same set of materials. These findings not only highlight the crucial role that an accurate engineering and

optimisation of the BL (in term of both materials and processing) plays in determining the final devices performances but demonstrate also the effectiveness of the P3HT based SDSC as an effective, reliable and cost effective alternative to conventional DSC technology.

Acknowledgments

We grateful thank Dr. Andrea Capasso at Queensland University Technology (Brisbane, Australia) for SEM images, Dr. Annamaria Petrozza (at Italian Institute of Technology (Milano, Italy), Giuseppe Costanzo (at C.H.O.S.E.), Prof. Pier Gianni Medaglia (at University of Rome Tor Vergata), Dr. Simone Mastroianni and Dr. Angelo Lembo (at Dyepower) for their helpful contribution.

This work was supported by a grant from Regione Lazio "Polo Solare Organico Regione Lazio."

References

1. B. O'Regan, B.; M. Grätzel, A low-cost, high-efficiency solar cell based on dye-sensitized colloidal TiO_2 films, Nature 353 (1991) 737-740.
2. B.E. Hardin; H.J. Snaith; M.D. McGehee, The renaissance of dye solar cells, Nature Photonics 6 (2012) 162-169.
3. A. Yella, H.W. Lee, H.N. Tsao, C. Yi, A.K. Chandiran, M.K. Nazeeruddin, E.W.G. Diau, C.Y. Yeh, S.M. Zakeeruddin, M. Grätzel, Porphyrin-Sensitized Solar Cells with Cobalt (II/III)–Based Redox Electrolyte Exceed 12 Percent Efficiency, Science 334 (2011) 629-634.
4. G. Mincuzzi, M. Schulz-Ruhtenberg, L. Vesce, A. Reale, A. Di Carlo, A. Gillner, T. M. Brown, Laser processing of TiO_2 film for dye solar cells: a thermal, sintering, throughput and embodied energy investigation, Progress in photovoltaics: Research and Applications (2012) DOI: 10.1002/pip.2261.
5. F. Giordano, E. Petrolati, T.M. Brown, A. Reale, A. Di Carlo, Series-connection designs for dye solar cell modules, IEEE Transactions on Electron Devices 58 (2011) 2759–2764.
6. S. Dai, K. Wang, J. Weng, Y. Sui, Y. Huang, S. Xiao, S. Chen, L. Hu, F. Kong, X. Pan, C. Shi, L. Guo, Design of DSC panel with efficiency more than 6%, Solar Energy Materials & Solar Cells 85 (2005) 447–455.
7. H. Arakawa, T.Yamaguchi, T. Sutou, Y. Koishi, N Tobe, D. Matsumoto, T. Nagai, Efficient dye-sensitized solar cell sub-modules Current Applied Physics 10 (2010) 157–160.

8. M.I. Asghar, K. Miettunen, J. Halme, P. Vahermaa, M. Toivola, K. Aitola, P. Lund, Review of stability for advanced dye solar cells, Energy Environ. Sci., 3 (2010) 418-426.
9. S. Mastroianni, A. Lanuti, S. Penna, A. Reale, T.M. Brown, A. Di Carlo, F. Decker, Physical and electrochemical analysis of an indoor-outdoor ageing test of large-area dye solar cell devices, Chem. Phys. Chem, 13 (2012) 2925-2936.
10. S. Mastroianni, A. Lanuti, T.M. Brown, R. Argazzi, S. Caramori, A. Reale, A. Di Carlo, Reverse bias degradation in dye solar cells, Applied Physics Letter, 101 (2012) 123302-123305.
11. S.A. Sapp, C.M. Elliott, C. Contado, S. Caramori, C.A. Bignozzi, Substituted polypyridine complexes of cobalt (II/III) as efficient electron transfer mediators in dye-sensitized solar cells. J. Am. Chem. Soc., 124 (2002) 11215–11222.
12. Z. Zhang, P. Chen, T.N. Murakami, S.M. Zakeeruddin, M. Grätzel. The 2,2,6,6-tetramethyl-1-piperidinyloxy radical: An efficient, iodine-free redox mediator for dye-sensitized solar cells. Adv. Funct. Mater., 18 (2008) 341–346.
13. P. Wang, S.M. Zakeeruddin, J.E. Moser, R. Humphry-Baker, M. Grätzel, A solvent-free, $SeCN^-$ /$(SeCN)_3^-$ based ionic liquid electrolyte for high efficiency dye-sensitized nanocrystalline solar cells, J. Am. Chem. Soc., 126 (2004) 7164–7165.
14. P. Wang, S.M. Zakeeruddin, J.E. Moser, M.K. Nazeeruddin, T. Sekiguchi, M. Grätzel, A stable quasi-solid-state dye-sensitized solar cell with an amphiphilic ruthenium sensitizer and polymer gel electrolyte, Nature Material, 2 (2003) 402-407.
15. U. Bach, D. Lupo, P. Comte, F. Weissortel, J.Selbeck, H. Spreitzer, M. Grätzel, Solid-state dye-sensitized mesoporous TiO2 solar cells with high photon-to-electron conversion efficiencies. Nature, 395, (1998) 583–585.
16. H.J. Snaith, A.J. Moule, C. Klein, K. Meerholz, R.H. Friend, M. Grätzel, Efficiency enhancements in solid-state hybrid solar cells via reduced charge recombination and increased light capture. Nano Letter, 7 (2007) 3372–3376.
17. H.J. Snaith, L. Schmidt-Mende, Advances in Liquid-Electrolyte and Solid-State Dye-Sensitized Solar Cells, Nano Letter, 19 (2007) 3187-3200.
18. J. Burschka, A. Dualeh, F. Kessler, E. Baranoff, N.L. Cevey-Ha, C. Yi, M.K. Nazeeruddin, M. Grätzel, Tris(2-(1H-pyrazol-1-yl)pyridine)cobalt(III) as p-type dopant for organic semiconductors and its application in highly efficient solid-state dye-sensitized solar cells, J. Am. Chem. Soc., 133 (2011), 18042–18045.
19. J. Melas-Kyriazi, I.K. Ding, A. Marchioro, A. Punzi, B.E. Hardin, G.F. Burkhard, N. Tétreault, M. Grätzel, J.E. Moser, M.D. McGehee, The effect of hole transport material pore filling on

photovoltaic performance in solid-state dye-sensitized solar cells, Advanced Energy Materials, 1, (2011) 407–414.

20. P. Docampo, A Hey, S. Guldin, R. Gunning, U. Steiner, H.J. Snaith, Pore filling of Spiro-OMeTAD in Solid-State Dye-Sensitized Solar Cells determined via optical reflectometry, Advanced Energy Materials, (2012) DOI: 10.1002/adfm.201201223.
21. N. Cai, S.J. Moon, N.L.Cevey-Ha, T. Moehl, R. Humphry-Baker, P. Wang, S.M. Zakeeruddin, M. Grätzel, An organic D-π-A dye for record efficiency Solid-State Sensitized Heterojunction Solar Cells, Nano Letters, 11 (2011), 1452-1456.
22. L. Schmidt-Mende, U. Bach, R. Humphry-Baker, T. Horiuchi, H. Miura, S. Ito, S. Uchida, M. Grätzel, Organic Dye for Highly Efficient Solid-State Dye-Sensitized Solar Cells, Advanced Materials, 17 (2005) 813-815.
23. H.J. Snaith, A. Petrozza, S. Ito, H. Miura, M. Grätzel, Charge generation and photovoltaic operation of Solid-State Dye-Sensitized Solar Cells incorporating a high extinction coefficient Indolene-based sensitizer, Advanced Functional Material, 19 (2009) 1810-1818.
24. I. Chung, B. Lee, J. He, R.P.H. Chang, M.G. Kanatzidis, All-solid-state dye-sensitized solar cells with high efficiency, Nature Letter, 485 (2012) 486-489.
25. R. Zhu, C.Y. Jiang, B. Liu, S. Ramakrishna, Highly efficient nanoporous TiO_2-Polythiophene Hybrid Solar Cells based on interfacial modification using a Metal-Free Organic Dye, Advanced Materials, 21 (2009) 994–1000.
26. W. Zhang, R. Zhu, F. Li, Q. Wang, B Liu, High-Performance Solid-State Organic Dye Sensitized Solar Cells with P3HT as Hole Transporter, J. Phys. Chem. C, 115 (2011) 7038-7043.
27. A. Abrusci, I.K. Ding, M. Al-Hashimi, T. Segal-Peretz, M.D. McGehee, M. Heeney, G.L. Freyd, J.H Snaith, Facile infiltration of semiconducting polymer into mesoporous electrodes for hybrid solar cells, Energ. Environ. Sci., 4 (2011) 3051–3058.
28. L. Yang, U.B. Cappel, E.L. Unger, M. Karlsson, K. M. Karlsson, E. Gabrielsson, L. Sun, G. Boschloo, A. Hagfeldt , E.M.J Johansson, Comparing spiro-OMeTAD and P3HT hole conductors in efficient solid state dye-sensitized solar cells, Phys. Chem. Chem. Phys., 14 (2012) 779-789.
29. J.A. Chang, J.H. Rhee, S.H. Im, Y.H. Lee, H.J. Kim, S.I. Seok, M.D. Nazeeruddin, M. Grätzel, High-performance nanostructured inorganic-organic heterojunction solar cells, Nano Letters, 10 (2010) 2609-2612.
30. L. Kavan, M. Grätzel, Highly efficient semiconducting TiO_2 photoelectrodes prepared by aerosol pyrolysis, Electrochim. Acta, 40 (1995) 643-652.
31. B. Peng, G. Jungmann, C. Jäger, D. Haarer, H.W. Schmidt, M. Thelakkat, Systematic investigation of the role of compact TiO2 layer in solid state dye-sensitized TiO2 solar cells,

Coordination Chemistry Reviews, 248 (2004) 1479-1489.

32. H. J. Snaith, M. Grätzel, The Role of a "Schottky Barrier" at an Electron-Collection Electrode in Solid-State Dye-Sensitized Solar Cells, Advanced Materials, 18 (2006) 1910-1914.
33. K. Miettunen, J. Halme, P. Vahermaa, T. Saukkonen, M. Toivola, P. Lund, Dye solar cell on ITO-PET substrate with TiO_2 recombination blocking layers, Journal of the Electrochemical Society, 156 (2009) B876-B883.
34. M.Wu, Z.H. Yang, Y.H. Jiang, J.J. Zhang, S.Q. Liu, Y.M. Sun, Improvement of dye-sensitized solar cell performance through electrodepositing a close-packed TiO2 film, J. Solid State Electrochem., 14 (2010) 857-863.
35. J.N. Hart,D. Menzies,Y.B. Cheng, G.P. Simon,L. Spiccia, TiO_2 sol–gel blocking layers for dye-sensitized solar cells, Comptes Rendus Chimie, 9 (2006) 622-626.
36. P.J. Cameron, L.Peter, Characterization of Titanium Dioxide Blocking Layers in Dye-Sensitized Nanocrystalline Solar Cells, J. Phys. Chem. B, 107 (2003) 14394-14400.
37. P.J. Cameron, L.Peter, How important is the back reaction of electrons via the substrate in Dye-Sensitized Nanocrystalline Solar Cells?, J. Phys. Chem. B, 109 (2005) 930-936.
38. H.J. Chen, L. Wang, W.Y. Chiu, Chelation and solvent effect on the preparation of titania colloids, Materials Chemistry and Physics, 101 (2007) 12–19.
39. P. Kajitvichyanukul, S. Pongpom, A. Watcharenwong, J. Ananpattarachai, Effect of Acetyl Acetone on Property of TiO2 Thin Film for Photocatalytic Reduction of Chromium(VI) from Aqueous Solution, Journal Special Issue on Nanotechnology, 4 (2005) 87-93.
40. W.R. McNamara, R.C. Snoeberger III, G. Li, J.M. Schleicher, C.W. Cady, M. Poyatos, C.A. Schmuttenmaer, R.H. Crabtree, G.W. Brudvig, V.S. Batista, Acetylacetonate anchors for robust functionalization of TiO_2 nanoparticles with Mn(II)-Terpyridine complexes, J. Am. Chem. Soc., 130 (2008) 14329-14338.
41. D.P. Hagberg, X. Jiang, E. Gabrielsson, M. Linder, T. Marinado, T. Brinck, A. Hagfeldt and L. Sun, Symmetric and unsymmetric donor functionalization. comparing structural and spectral benefits of chromophores for dye-sensitized solar cells, J. Mater. Chem., 19 (2009) 7232-7238.
42. H.J. Snaith, How should you measure your excitonic solar cells?, Energy Environ. Sci., 5 (2012) 6513-6520.
43. Y.Djaoued, S. Badilescu, P.V. Ashrit, D. Bersani, P.P. Lottici, J. Robichaud, Study of anatase to rutile phase transition in nanocrystalline titania films, Journal Sol-Gel Science and Technology, 24 (2002) 255-264.
44. F.D. Hardcastle, Raman Spectroscopy of Titania (TiO_2) Nanotubular Water-Splitting Catalysts, Journal of the Arkansas Academy of Science, 65 (2011) 43-48.
45. S.W. Boland, S.C. Pillai, W.D. Yang and S.M. Haile, Preparation of (Pb,Ba)TiO_3 powders and highly oriented thin films by a sol-gel process, J. Mater. Res., 19 (2004) 1492-1498.

46. H.J. Chen, L. Wang, W.Y. Chiu, Chelation and solvent effect on the preparation of titania colloids, Materials Chemistry and Physics 101 (2007) 12–19.
47. E.M.J. Johansson, S. Pradhan, E. Wang, E.L. Unger, A. Hagfeldt, M. R. Andersson, Efficient infiltration of low molecular weight polymer in nanoporous TiO_2, Chemical Physics Letters, 502 (2011) 225–230.
48. F. Fabregat-Santiago, J. Bisquert, G. Garcia-Belmonte, G. Boschloo, A. Hagfeldt, Influence of electrolyte in transport and recombination in dye-sensitized solar cells studied by impedance spectroscopy, Solar Energy Materials and Solar Cells, 87 (2005) 117-131.

Figure captions

Fig. 1. Batch (i): Relative variations of the main photovoltaic parameters (V_{oc}, J_{sc}, FF, PCE) extracted from cells with a ACAC BL respect to cells with a conventional BL are reported. Measurements were carried out on masked devices (0.25 cm^2 active area) under AM 1.5 and 1 sun illumination conditions with a class A sun simulator (Abet 2000) calibrated with a Skye SKS 1110 sensor.

Fig. 2. For devices with ACAC-BL, average PCE values vs. the number of spray cycles *n* are shown. Values are reported normalized to the PCE maximum correspondent to $n = 15$. Black squares are relative to batch (ii) devices obtained varying *n* over a large interval (from $n = 0$ to $n = 50$) whilst red asterisk are relative to batch (iii) devices where *n* was varied over a more restricted interval (from $n = 5$ to $n = 20$).

Fig. 3. The SEM cross section of the c-TiO_2 layer (deposited over the Glass/FTO substrate) obtained after $n = 15$ spray cycles of a precursor solution containing ACAC is reported. The c-TiO_2 thickness is shown to be nearly 100 nm (black bar).

Fig. 4. SEM cross-section of the nc-TiO_2 film after dyeing and P3HT filling. Black dashed circles indicate a well uniformly distributed quasi continuous network of large aggregates with size of some hundreds of nanometers identified as the infiltrated P3HT interpenetrating the nc-TiO_2 film (which in turn is composed of distinguishable nanoparticles with a size of around 20 nm).

Fig. 5. Batch (iii): I_0 (red squares), β_a (black triangles) and β_c (green circles) values vs. the number of spray cycles *n* are shown. Respect to $n = 0$ (i.e. no BL), for $n = 15$, a lower I_0 and higher β_c values, are observed, whilst is the β_a value unchanged. For $15 < n \leq 50$, I_0 and β_c values didn't show remarkable variations respect to $n = 15$ whilst β_a is observed to sensibly increase only for $n \geq 30$.

Fig. 6. EIS spectra of symmetric cells relative to Batch (vii) are reported. Cells with BLs were fabricated varying the number of spray, *n,* for both a conventional (open squares) and ACAC (open triangles) c-TiO_2 precursor formulation. Also reported the equivalent model circuit $R_s(R_{ct}{\cdot}Q)$ utilised to fit the EIS measurements. The percentage of the electrode FTO surface left uncovered after the BL fabrication has been reported vs. *n* for both a conventional (open squares) and ACAC (open triangles) c-TiO_2 precursor formulation.

Fig. 7. Average PCE values extracted from cells of batches (iv), (v) and (vi) are shown. All batches

were fabricated utilising the optimized BL (utilising TAA/ACAC in ethanol and n =15 spray cycles) and the same set of materials. Measurements were carried out on masked devices (0.25 cm^2 active area) under AM 1.5 and 1 sun illumination conditions with a class A (Abet 2000) sun simulator calibrated with a Skye SKS 1110 sensor.

Fig.8. IPCE spectrum relative to a representative cell of batch (v) showing (under 1 sun, illumination, Class A sun simulator condition) a PCE = 3.9% (see the graph inset). A value of J_{sc} =6.7 mA/cm^2 can be calculated integrating the IPCE spectrum from λ_1=300 nm to λ_2=800 nm. The value extracted from measurements under the sun simulator was J_{sc} =7.2 mA/cm^2 (see the inset graph).

Fig. 9. J-V measurement of the best cell fabricated (batch (v)). Measurement was carried out on masked device (0.25 cm^2 active area) under AM 1.5 and 1 sun illumination conditions with a class A sun simulator (Abet 2000) calibrated with a Skye SKS 1110 sensor.

Tab. 1 Characteristic Tafel plot parameters extracted from devices of batch (i) are reported. Values relative to both devices fabricated with ACAC-BL and a conventional BL are compared.

	I_0 [A]	β_a [mV/dec]	β_c [mV/dec]
Without ACAC	$1.0 \cdot 10^{-6}$	231	464
With 0.4M ACAC	$8.2 \cdot 10^{-8}$	198	467

Tab.1

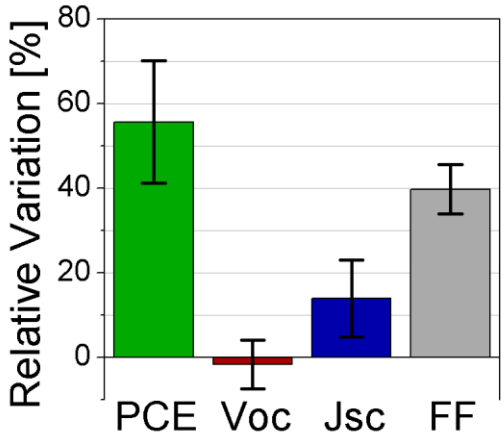

Fig. 1.

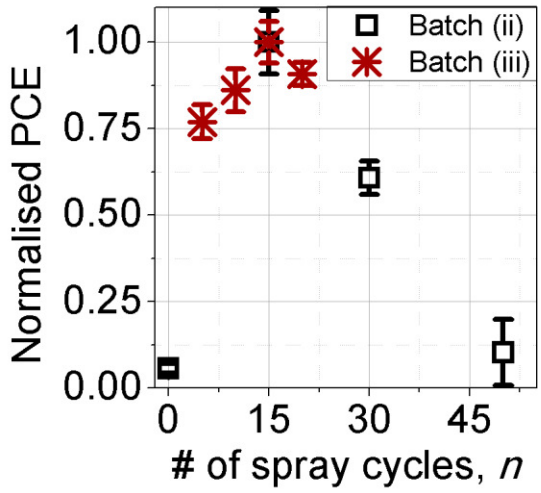
Batch (ii)
Batch (iii)
Normalised PCE
1.00
0.75
0.50
0.25
0.00
0
15
30
45
# of spray cycles, n

Fig. 2.

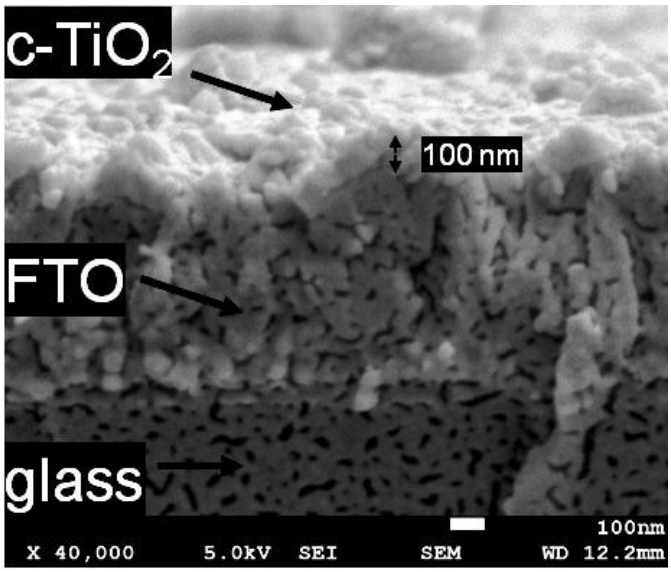
c-TiO2
100 nm
FTO
glass
100nm
X 40,000
5.0kV
SEI
SEM
WD 12.2mm

Fig. 3.

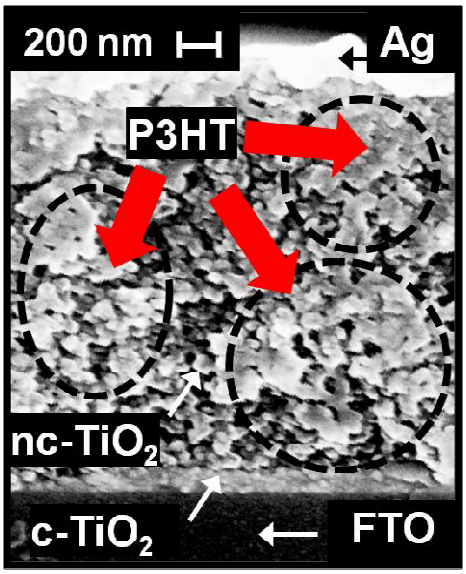
200 nm
Ag
P3HT
nc-TiO2
c-TiO2
FTO

Fig.4

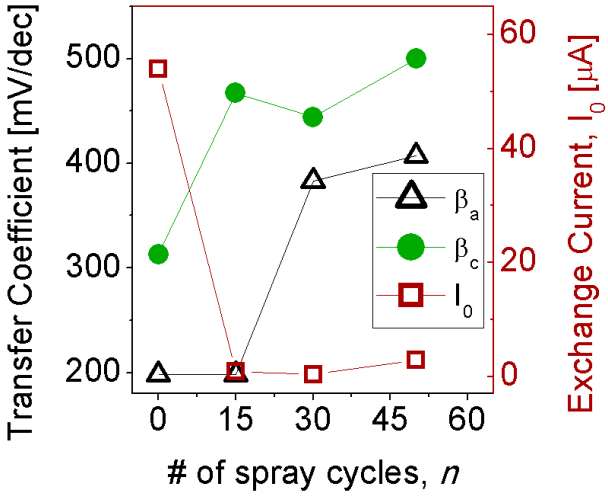
Transfer Coefficient [mV/dec]
500
400
300
200
0
15
30
45
60
# of spray cycles, n
60
40
20
0
Exchange Current, I0 [μA]
βa
βc
I0

Fig.5

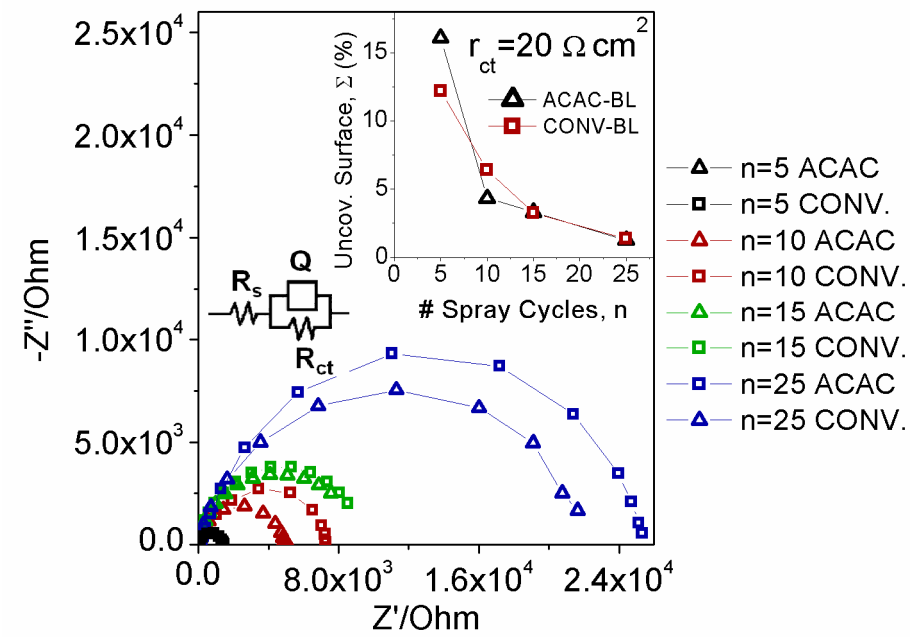
2.5x10^4
2.0x10^4
1.5x10^4
1.0x10^4
5.0x10^3
0.0
-Z''/Ohm
0.0
8.0x10^3
1.6x10^4
2.4x10^4
Z'/Ohm
Q
R_s
R_ct
Uncov. Surface, Σ (%)
15
10
5
0
0
5
10
15
20
25
# Spray Cycles, n
r_ct =20 Ω cm^2
ACAC-BL
CONV-BL
n=5 ACAC
n=5 CONV.
n=10 ACAC
n=10 CONV.
n=15 ACAC
n=15 CONV.
n=25 ACAC
n=25 CONV.

Fig. 6.

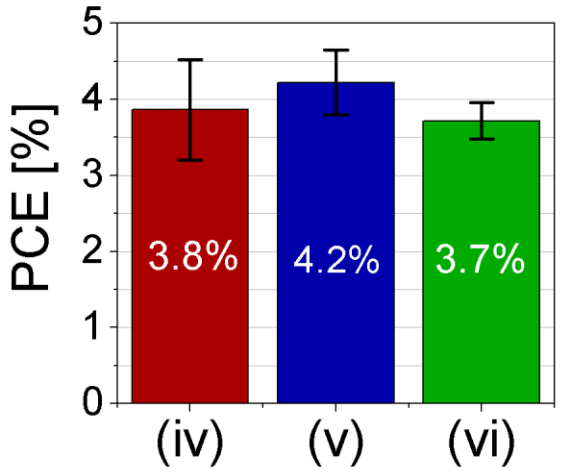
PCE [%]
5
4
3
2
1
0
3.8%
4.2%
3.7%
(iv)
(v)
(vi)

Fig. 7

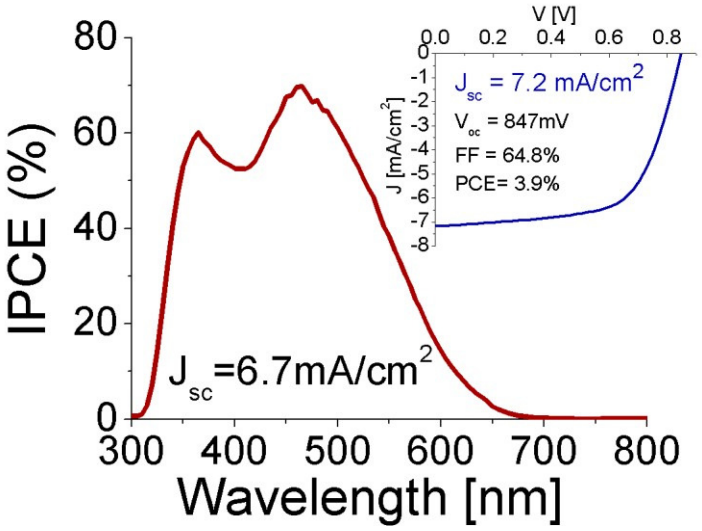
IPCE (%)
Wavelength [nm]
J_sc=6.7mA/cm^2
V [V]
J [mA/cm^2]
J_sc = 7.2 mA/cm^2
V_oc = 847mV
FF = 64.8%
PCE= 3.9%

Fig. 8

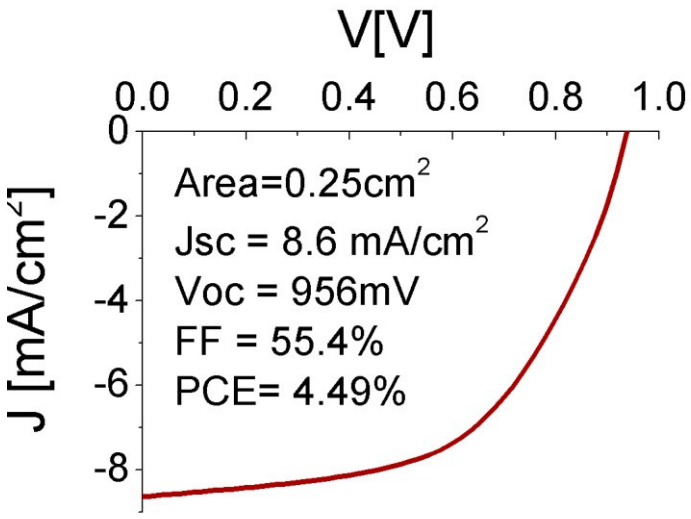
V[V]
J [mA/cm^2]
Area=0.25cm^2
Jsc = 8.6 mA/cm^2
Voc = 956mV
FF = 55.4%
PCE= 4.49%

Fig. 9